Geologia Croatica
Journal of the Croatian Geological Survey and the Croatian Geological Society
2022 | 75/2 | 211–222| 8 Figs. | www.geologia-croatica.hr

The origin of a complex breccia body within the Upper Cretaceous/Early Eocene succession on Pag Island (Karst Dinarides, Croatia): karstic dissolution and collapse or dilational faulting and collapse origin?

Dražen Kurtanjek*, Damir Bucković, Darko Tibljaš and Blanka Cvetko Tešović

Department of Geology, Faculty of Science, University of Zagreb, Horvatovac 102a, HR-10000 Zagreb, Croatia; (*corresponding author: drkurtan@geol.pmf.hr)

doi: 10.4154/gc.2022.15

Article history:
Manuscript received September 10, 2021
Revised manuscript accepted February 14, 2022
Available online June 23, 2022

Keywords: breccia, karstic dissolution, dilational faulting, Upper Cretaceous, Pag Island, Karst Dinarides

Abstract

A kilometre west of Pag Town on Pag Island, Croatia, within the Upper Cretaceous shallow-water carbonate succession, there is a large breccia body that has an irregular, quasi-circular shape and a subvertical-oblique position in relation to the bedding of the host rock. The breccia clasts and fragments consist almost entirely of the Upper Cretaceous host rock with only sporadic clasts of the Lower Eocene foraminiferal (alveolinid) limestones. In the brecciated body, there are three breccia types. 1) crackle breccia, 2) mosaic breccia, and 3) chaotic breccia. Based on the textural and structural characteristics of these types of breccia such as chaotic appearance and random fabric, very poorly sorted material, angular fragments, the composition reflecting only the host rock lithology, two genetic scenarios or concepts for the origin of Pag Town breccia body were considered, with observations supporting each of them. The first concept involves host rock dissolution resulting in a widened dissolution cavity into which wall and roof rocks progressively collapsed, and the second concept involves the collapse of voids produced by dilational fault displacement. A common prerequisite to both opposing scenarios is the existence of a subsurface cavity or void where the accumulation of rock clasts and fragments occurred. It is assumed that the timing of the cavity formation is related mainly to karstification during the Late Cretaceous-Early Eocene emersion phase or is related to dilational faulting during the Palaeogene Dinarides thrusting event.

1. INTRODUCTION

Breccia is a term used for a rock body that consists of a variety of individual clasts and fragments, which are commonly very angular and may have a fine-grain matrix and/or be cemented together by a mineral cement. The grains within the matrix may not have a similar composition to those of the rock fragments (LAZNICKA, 1988; SCHOLZ, 1990). The origin of some breccias can be deduced from their texture, composition, and context (i.e., position within the brecciated body), but the origin or the three-dimensional geometry of other breccias is often uncertain. One problematic breccia formation mechanism is the gravitational collapse into voids formed either by dissolution (LOUCKS, 1999), or by a mismatch of fault walls (e.g. WOODCOCK et al., 2006; FERRILL et al., 2011; WALKER et al., 2011). The Pag Town breccia body exposed west of Pag Town on the island of Pag (Fig. 1) highlights this dilemma. The stratigraphic position of the breccia is very close to the top of the Upper Cretaceous shallow-water carbonate succession capped with two unconformities; the older one which represents a regional emersion event lasting from the Late Cretaceous till the Early Eocene (e.g., DURN et al., 2003; OTONIČAR, 2007; KORBAR, 2009; BRLEK et al., 2013; PEH & KOVAČEVIĆ GALOVIĆ, 2016), and a younger emergence event, occurring during the Early Eocene that was much shorter but of indeterminate duration (a few millions of years?). Both unconformities indicate long-term exposure during which karstification could develop in the relatively near-surface sections. For example, as the fractures in the exposed surfaces were enlarged over time by chemical dissolution, more flow is directed into the fractures. The fracture conductivity increases by several orders of magnitude with increasing fracture width. Consequently, flow in a mature karst aquifer is characterized by efficient drainage through the fractures, which, when sufficiently enlarged, become cave systems (KAUFMANN & BRAUN, 2000). Alternatively, the presence of easily recognizable fault zones in the study area may also indicate the grinding action of two fault blocks as they slide past each other forming a dilational-fault void that underwent subsequent collapse. The objective of this investigation is to describe the structural setting and the composition, texture, and fabric of this breccia body and provide observations related to two postulated origins that can be used to suggest an interpretation of the genesis of the breccia body.

2. GEOLOGICAL SETTING

The island of Pag is situated in the north-eastern part of the Adriatic Sea (Fig. 1). The area is characterized by gentle folds, striking in the northwest, Dinaridic direction (MAJCEN et al., 1970). The fold limbs are refolded and faulted by local strike-slip fault systems. Geomorphologically, the observed anticlines correspond to the elongated upland ridges and highs, while the synclines correspond to the narrow, shallow karstic valleys. The anticlines are composed of Upper Cretaceous rudist limestones and dolomites, and Lower – Middle Eocene foraminiferal limestones. The synclines are filled with Middle–Upper Eocene flysch clastics, sandstones, and marls, and are covered by the Quaternary deposits (see MAJCEN et al., 1970; MAMUŽIĆ et al., 1970; SOKAČ et al., 1974 for details). The island of Pag is located along

the NE Adriatic coast, which is a part of the Adriatic Carbonate Platform (AdCP - VLAHOVIĆ et al., 2005, also referred to as the Adriatic–Dinaridic Carbonate platform – ADCP – JENKYNS, 1991; GUŠIĆ & JELASKA, 1993; PAMIĆ et al., 1998; JELASKA, 2003), being one of the largest Mesozoic and most long-lasting carbonate platforms in the Mediterranean region.

The AdCP comprises a 4–6.5 km thick succession of almost pure carbonate rocks deposited from the Early Jurassic to the end of the Cretaceous (VLAHOVIĆ et al., 2005). It represents a significant part of the thicker succession (in places more than 8 km thick; TIŠLJAR et al., 2002; VELIĆ et al., 2002; VLAHOVIĆ et al., 2005) of mostly carbonate strata, which today form the Karst Dinarides (or External Dinarides), with a stratigraphic range of more than 300 Ma (the oldest outcrops are of Carboniferous age; RAMOVŠ et al., 1990; TEMKOVA, 1990; SREMAC, 2005). This succession was originally deposited on the Adria Microplate, which represented a promontory of Africa during the Mesozoic (CHANNELL et al., 1979; SCHMID et al., 2008 and references therein). The succession is now incorporated into a complex imbricated thrust and fold belt characterized mostly by SW vergences, extending for more than 600 km along the NE Adriatic coast (KORBAR, 2009 and references therein). By the end of the Cretaceous, large areas of the platform emerged, and the area of deposition on the platform gradually reduced (DURN et al., 2003; OTONIČAR, 2007; KORBAR, 2009; BRLEK et al., 2013; PEH & KOVAČEVIĆ GALOVIĆ, 2016, and references therein). At the end of the Cretaceous, a regional emergence took place, followed by karstification and sporadic bauxite formation. Transgressive Lower Eocene foraminiferal limestones with evidence of sporadic emersion events commonly overlie this regional erosional surface recording foreland basin deposition of foraminiferal limestones on a carbonate ramp with progressive deepening and transition into flysch-type deposition (DROBNE et al., 1991; KOŠIR, 1997; MARJANAC & ĆOSOVIĆ, 2000; VLAHOVIĆ et al., 2005; BABIĆ & ZUPANIČ, 2016 and references therein).

3. METHODS

Fieldwork included detailed mapping of the study area at 1:25000 scale and sampling breccia fragments for microscopic analyses and facies-type characterization. A petrographic study of thin-sections was done using plane-polarized transmitted light. Rock slabs and thin-sections were stained using a mixture of Alizarin red S and potassium ferricyanide dissolved in a dilute hydrochloric acid solution in order to differentiate carbonate minerals (DICKSON, 1966; EVAMY, 1969). Three breccia samples, four individual clasts samples separated from breccia, and four host rock samples were treated with 3.4% hydrochloric acid aiming to determine their insoluble residue content. X-ray powder diffraction (XRPD) analyses were performed on the insoluble residue of these samples and on one sample of the breccia matrix using a Philips PW3040/60 X'Pert PRO diffractometer equipped with Cu tube (40 kV and 40 mA) and proportional counter. Given the small quantity of material, Si zero-background sample holders on the spinner stage were used in parallel beam geometry (multilayer parabolic X-ray mirror). The relatively large iron content resulted in the high background, therefore several samples that were available in greater quantity (necessary for classic Al-holders) were also scanned with divergent beam geometry that included a graphite monochromator. In this case, the following slits were used: mask 10 mm, 1/2° divergence slit, 1° and 2° antiscat-

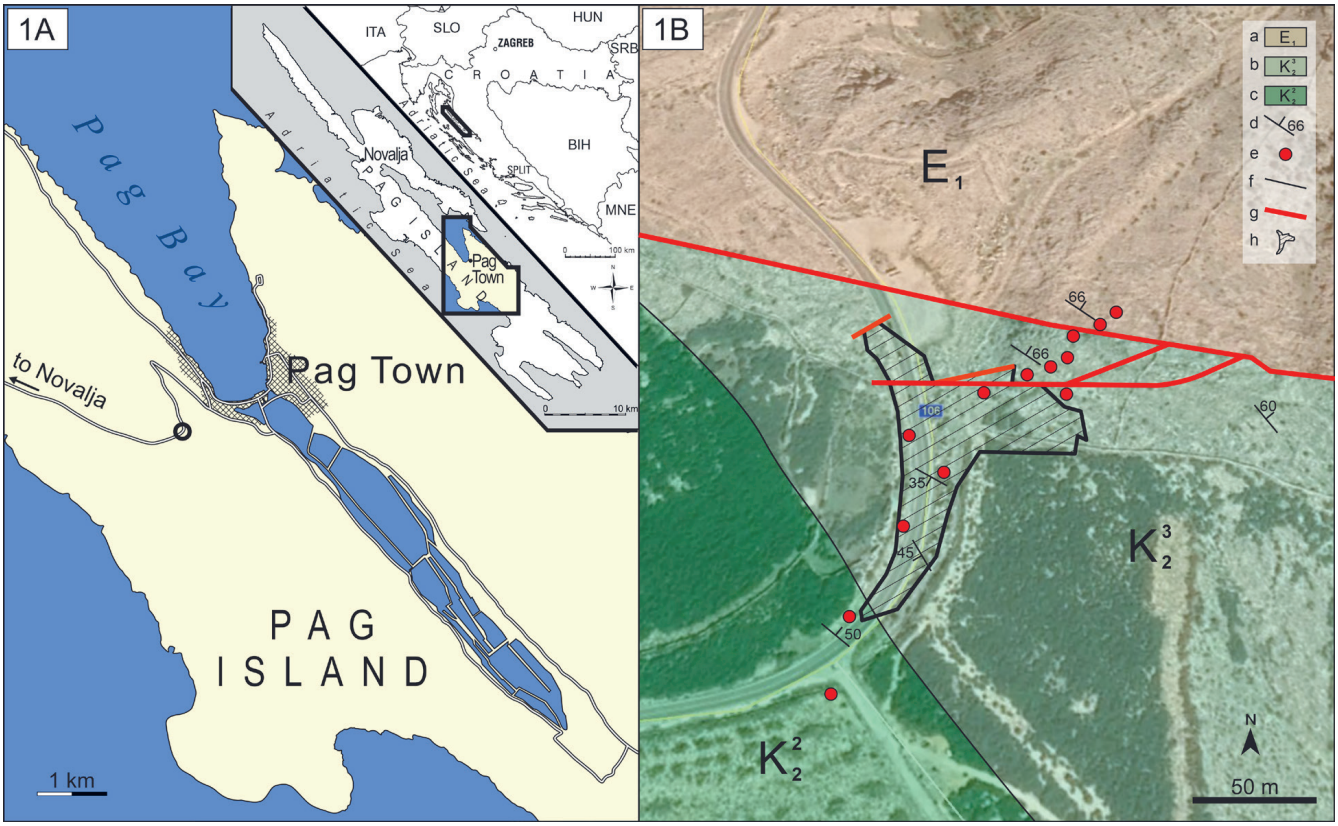

Figure 1. (A) Location map with the geographic position of the Pag Town breccia outcrop (circle) (Coordinates: 44° 26′ 14.19″ N, 15° 02′ 15.96″ E) and (B) Simplified geological map of the study area. Legend: a) E_1 – Lower Eocene, b) K_2^3 – Coniacian-Lower Campanian, c) K_2^2 – Upper Turonian, d) strike and dip (notice the difference between dip and dipping direction of the surrounding host rock contrary to those of blocks within the breccia body), e) sampling positions, f) geologic boundary, g) faults, h) breccia body

ter slits on the tube and detector side respectively, and a 0.2 mm receiving slit. The samples were scanned in continuous mode at a speed of 0.02°2θ/s. Diffraction patterns were processed using the X'Pert HighScore computer program (PANALYTICAL, 2004) and compared with the Powder Diffraction File database and with data from the literature (BROWN, 1961; BRINDLEY & BROWN, 1980; MOORE & REYNOLDS, 1997).

4. STRATIGRAPHIC POSITION

In the outcrop area, west of Pag Town (Fig. 1), a 97 m thick section of the breccia occurs within the Uppermost Turonian to Lower Campanian carbonate succession (Figs. 1B and Fig 2). The breccia body generally has irregular margins to the adjacent Upper Cretaceous host rock. In the lower section of the host rock, the limestone succession containing the breccia body is bioclastic wackestone/packstone/floatstone, composed of angular to subrounded bioclasts mainly derived from rudistid and other bivalves. The surrounding carbonate matrix generally contains calcareous dinoflagellate cysts (calcispheres, pithonellas) and various other fine-grained bioclasts such as echinoderm fragments, pelagic crinoids, sponge spicules, and echinoid spines. Such bio- and lithofacies characteristics can be correlated with the upper part of the Sveti Duh Formation, originally described from the Island of Brač (GUŠIĆ & JELASKA, 1990), and represent the gradual recovery of shallow-platform environments after a drowned phase during the Lower Turonian. Overlying these deposits are light gray to reddish-brown, moderately recrystallized mudstone and bioclastic wackestone/packstone/grainstone/floatstone limestone types, with various indeterminable miliolids, ataxophragmiids, rotaliids, thaumatoporellaceans (*Thaumatoporella parvovesiculifera* (RAINERI)), calcimicrobes (*Decastronema kotori* (DE CASTRO)), rudist (Radiolitidae), echinoderm and gastropod fragments, ostracods, peloids and intraclasts. Rare irregular fenestrae are also common. Among the foraminifera, the most common are; *Scandonea samnitica* DE CASTRO, *Pseudocyclammina sphaeroidea* GENDROT, *Cretaciclavulina gusici* SCHLAGINTWEIT & CVETKO TEŠOVIĆ, *Montcharmontia compressa* DE CASTRO, *Nezzazatinella picardi* (HENSON) and *Psudonummoloculina* spp. Such bio- and lithofacies indicate that these limestones were deposited in shallow subtidal environment, corresponding to the typical Gornji Humac formation (GUŠIĆ & JELASKA, 1990). Therefore, the stratigraphic position of the host rock limestone succession surrounding the breccia body can be defined within the time interval from the Late Turonian to Early Campanian (from ca. 87 to 80 Ma).

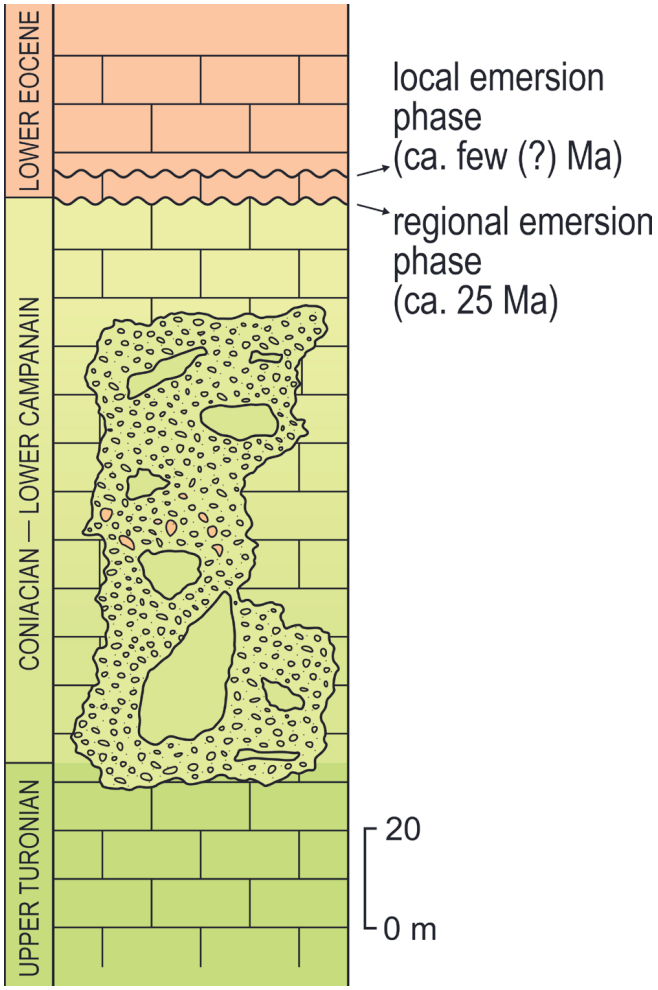

Figure 2. Simplified geological column showing the occurrence of the breccia body within the Upper Cretaceous succession.

5. BRECCIA FEATURES

The breccia body geometry is irregular, quasi-circular, and is oriented subvertically-obliquely to the bedding of the host rock (Fig. 1B). The northern, uppermost margin of the breccia body is faulted, revealing a straight contact plane with the Upper Cretaceous host rock (Fig. 1B). These faults have approximately E - W to NE - SW strikes and are almost vertical. Higher in the succession, at the Cretaceous - Early Eocene contact, there is a major left-lateral strike-slip fault striking NW - SE (Fig. 1B).

The breccia fragments are almost entirely composed of the surrounding host rocks, containing the same microfossil association. In chaotic breccias in several areas near the central part of the breccia body, sporadic pebble-sized fragments of Lower Eocene foraminiferal (alveolinid) limestone are noted (Fig. 2). The breccia fragments range in size between a few millimetres to more than two metres diameter. Many of the clasts can be designated as blocks (Fig. 3A), slabs (Fig. 3B), and chips (Fig. 3C). DAVIES (1949) and WHITE & WHITE (1969) defined blocks as masses of rock that still show bedding, slabs as fragments of single beds, and chips as bits of bedrock. The dip directions (from 200°–250°) of the blocks are different and even opposite to the dip directions of host rock strata (40°) (see in Fig. 1B). Clast shape is variable, but elongated and equidimensional clasts are the most common (Fig. 3). Roundness is low, with most clasts being angular to subangular, while in the stratified parts of the breccia the clasts may be subrounded to rounded (Fig. 4A).

Throughout the breccia body, the breccia fragments can be observed in different interrelationships. Therefore, the observed breccia fabrics can be classified into non-genetic breccia categories proposed by LOUCKS & HANDFORD (1992), as well as in those of LOUCKS (1999) for cave-collapse zones, or into the categories modified by MORT & WOODCOCK (2008), WOODCOCK & MORT (2008) for fault zone breccias. These categories include: (1) crackle breccia when the rock is highly fractured with thin fractures separating breccia clasts (Fig. 3D); (2) mosaic breccia; when displacement between clasts is greater and some of the clasts are rotated (upper part of Fig. 3E); this type includes both matrix-free and matrix-rich varieties. The crackle breccia, and mosaic breccia are present at the edges of the breccia body and are monomictic, that is they contain fragments of just one type of the host limestone. (3) chaotic breccia, is characterized by a predominantly polymictic composition and extensive rotation and displacement of clasts derived from different surrounding beds.

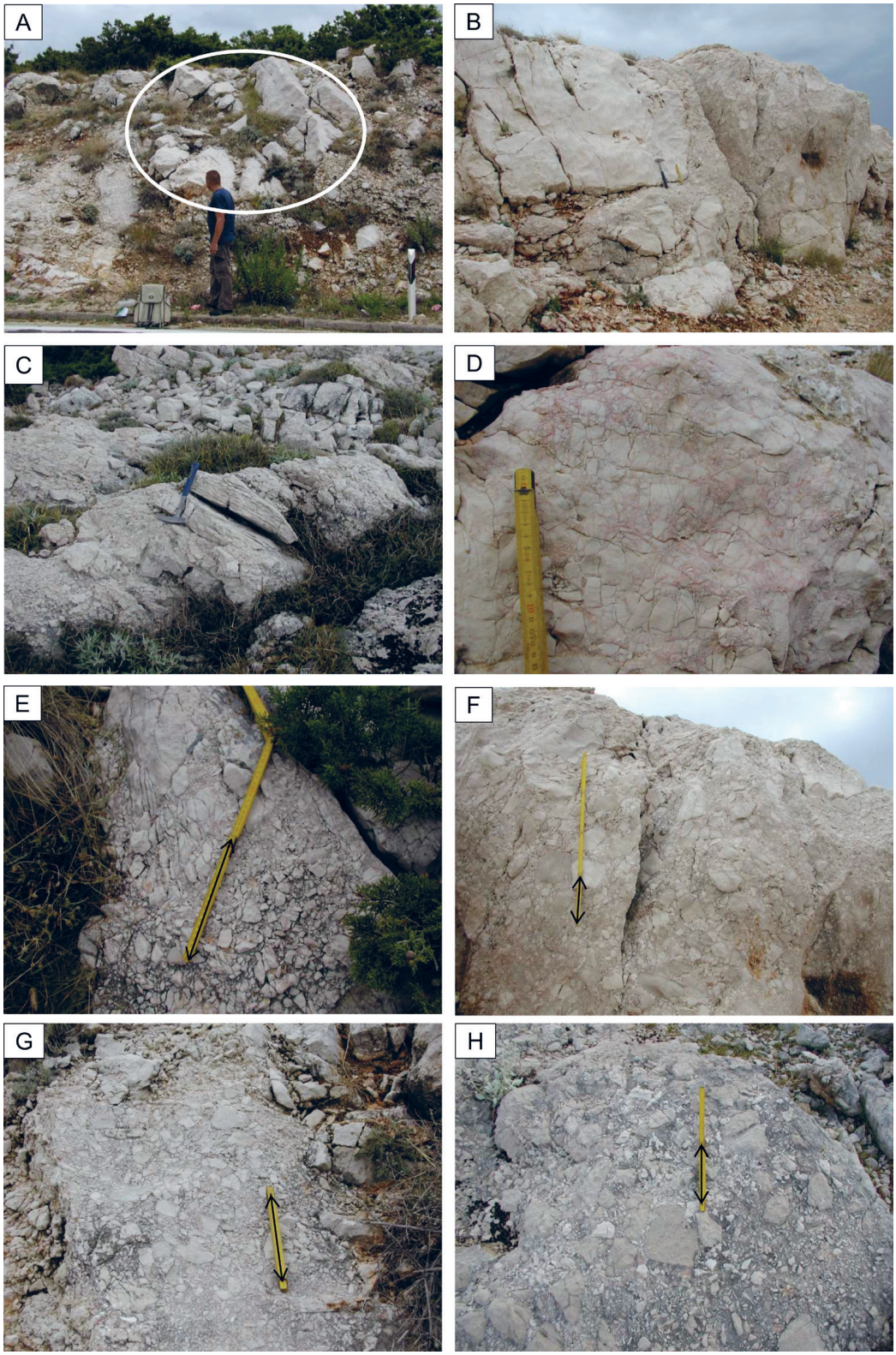

Figure 3. Examples of the characteristic types of breccia-fragments and non-genetic categories of the studied breccia: (A) Block – a mass of rock that still shows bedding (marked with an ellipse) representing a rotated fragment of host rock within chaotic breccia. The dip direction of layers in this block (200°) is opposite to the dip direction of layers in the host rock (40°); Person in front for scale 185 cm tall. (B) Slab – a fragment of a single bed (more than 2m long) within a coarse-clast chaotic breccia. (C) Chip – coarse-clast chaotic breccia fragment representing a bit of host rock; (B) and (C) rock hammer for scale (35 cm long). (D) Crackle breccia – highly fractured host rock with thin fractures separating breccia clasts. There is no displacement or any sign of transport of clasts. Note monomictic composition and tight fitting of clasts and noticeable reddish colouration. The small area (upper left) displays some more chaotic clasts organization. (E) Mosaic breccia – displacement between the clasts is greater than in crackle breccia. Some of the clasts have been rotated but the fitting is still recognizable. There is a transition from crackle breccia (upper part of the photo) to mosaic breccia (lower part of the photo). Both types of breccia are monomictic. (F) Chaotic breccia – internally disorganized polymictic breccia. Clasts have been rotated and translated enough to obscure any match with each other. Chaotic breccia appears as matrix free clast-supported (B, F), matrix-rich clast-supported (G), and matrix-supported type (H). Clasts shape varies from elongated to equidimensional, roundness is low with most clasts being subangular to angular (B, F, G, H). Coarse-clast chaotic breccia (A–C, F) belongs to one of six basic cave facies recognized in a palaeocave system (proposed by LOUCKS & MESCHER, 2001) interpreted as collapsed-breccia cavern fill characterized by a mass of very poorly sorted granule- to boulder- sized fragments of surrounding rocks that host the breccia. (E), (F), (G), (H) double-arrow line for scale 20 cm.

Clasts within the chaotic breccia have been rotated and translated to a point sufficient to obscure any match with each other (Figs. 3B, C, F). The chaotic breccia appears as a matrix free clast-supported breccia (Figs. 3B, F), matrix rich clast-supported breccia (Fig. 3G), and a matrix-supported breccia (Fig. 3H). The matrix within the matrix-rich type of breccia is a mixture of fine- to micro-breccia material (fine breccia - equals fragment sizes between 1–5 mm, SPRY, 1969; micro-breccia - equals average clasts size of 0.2 mm, HIGGINS, 1971), and detrital calcite silt. Clast-supported chaotic breccia prevails; it occupies the lower half and some of the upper parts of the breccia body, while the matrix-supported chaotic breccia appears only as a narrow zone within the upper half of the breccia body. Some breccias show stratification defined by clast shape and size, with lineation and poor development of imbricated pebbles (Fig. 4A). Other breccias show obstacle marks (Fig. 4F), and some show a ribbon to tabular-shaped breccia body, characterized by an irregularly undulating top and inversely graded clasts (Fig. 4B). The dip of the brecciated strata is not parallel with the host rock stratification.

Fitted fabric, convex-concave, and sutured contacts between the grains and wavy stylolites with iron oxide-stained pressure-dissolution seams are very common features of the breccia (Figs. 4C, 5A).

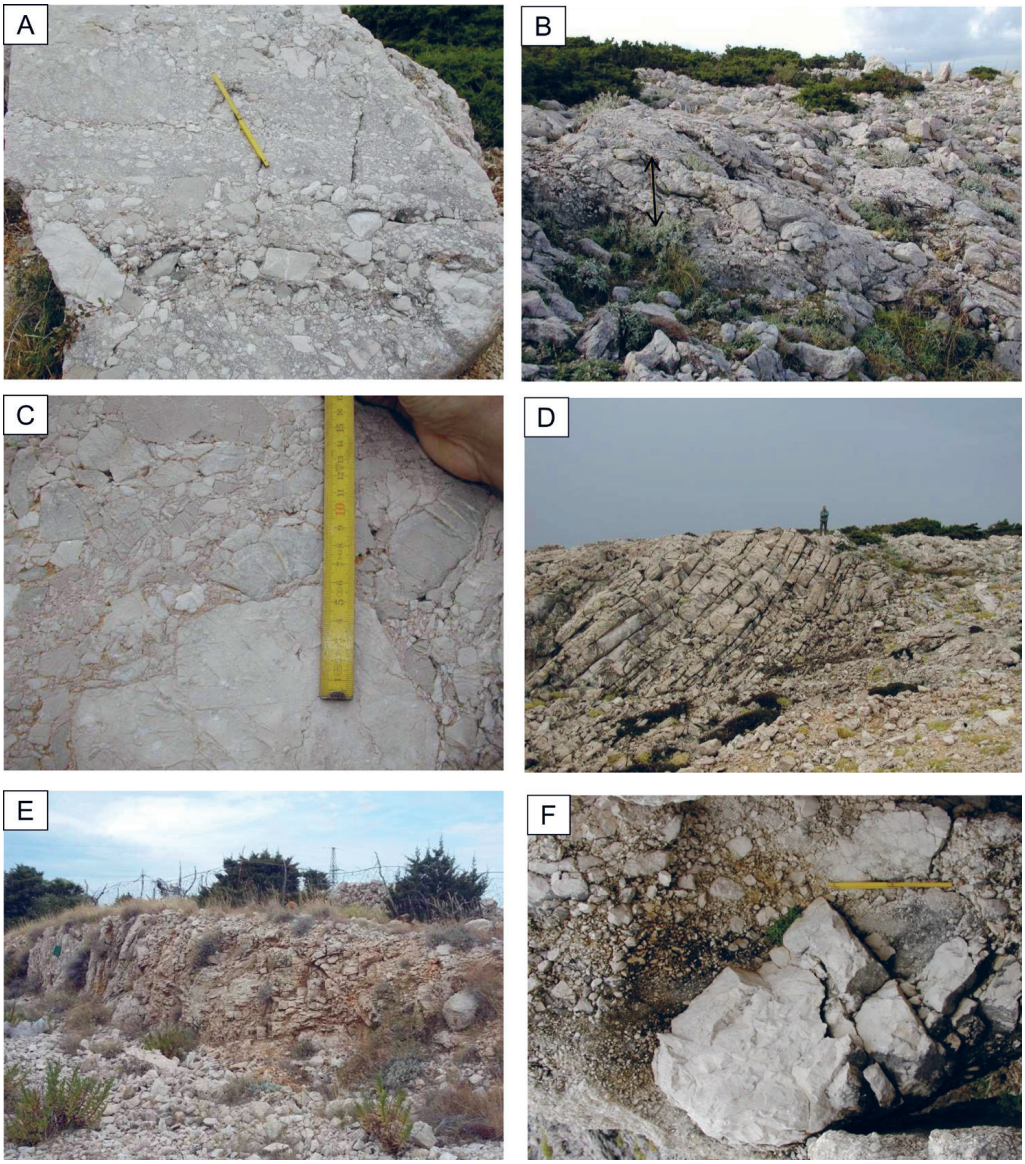

Figure 4. Facies determined in the studied breccia that match the basic palaeocave facies proposed by LOUCKS & MESCHER (2001) (A, B, D, E) and some specific textural-structural features of the breccia (C, F): (A) Finer-clast breccia displaying crude packaging and stratification defined by clast shape and size interpreted as hydrodynamically sorted, transported-breccia cavern fill. Some pebbles show lineation and poorly developed imbrication and are mostly subrounded to rounded; meter for scale 42 cm. (B) Inversely graded coarse-clast chaotic breccia displaying ribbon to tabular shaped body with the irregular, undulating top representing another variety of the same facies shown in Fig. 3A–C, F–H; double-arrow line for scale 90cm. (C) Detail of chaotic breccia showing common fitted fabric, concave-convex and sutured contact between the grains, and fine-breccia material between larger clasts. Reddish-brown fine-grained pore filling sediment is insoluble residue material. (D) Host rock strata with visible bedding continuity; for scale-man in the picture is 185 cm tall. Dip direction and dip: 40/66 (E) Disturbed host rock strata. The bedding is visible but is folded and offset by small faults; the notebook at the left part of the outcrop is 20 cm long and 14.5 cm wide for scale. Dip direction and dip: 40/45. (F) Detail of chaotic breccia showing obstacle mark, a structure formed by secondary currents which originate when the main streamflow is obstructed by obstacles within the path of the current. Coarse particle (boulder in the centre) was anchored to the bottom, the current was not able to remove it, and a shadow zone (upper left) is created by its protrusion. Smaller particles can find protection in the shadow zone, where turbulence and velocity are reduced, and come to rest; meter for scale 42 cm.

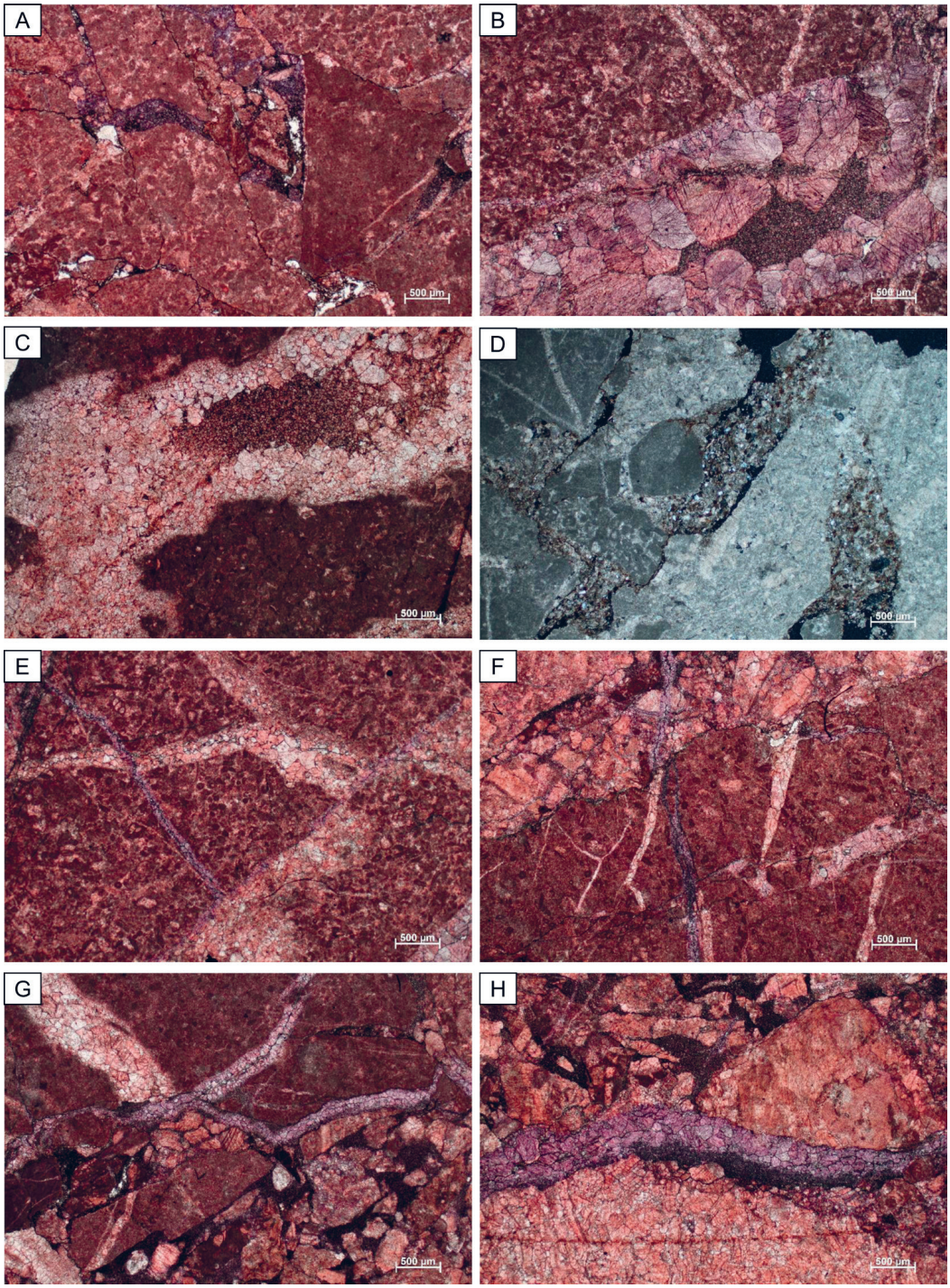

Figure 5. (A) Fitted fabric resulting from strong mechanical and chemical compaction. Wavy and sutured, microstyloltitic contacts between the grains are lined with the pressure-dissolution seams. Original pores are filled with detrital/crystal ferroan calcite silt. Plane-polarized light. Stained with Alizarin red S and K-ferricyanide. (B) Typical breccia pore-filling cement. The calcite spar has a well-developed drusy mosaic fabric characterized by an increasing crystal size towards the centre of the cavity. Detrital and crystal calcite silt fill the inner, uncemented pore space. Both calcite spar and crystal silt turn blue after treatment with Alizarin red S and K-ferricyanide indicating ferroan calcite with a late diagenetic, burial origin. Plane-polarized light. Stained with Alizarin red S and K-ferricyanide. (C) Microkarstic dissolution-cavity filling pattern similar to (B) but here, the drusy calcite spar and crystal silt have a non-ferroan composition (red colouration after staining) indicating an origin during early, near-surface diagenesis of microkarstic dissolution and cementation. This type of cavity-infill with non-ferroan calcite spar and detrital calcite silt occurs solely within the clasts and were formed in the original sediment i.e. in the surrounding breccia-host rock prior the brecciation. Plane-polarized light. Stained with Alizarin red S and K-ferricyanide. (D) Example of breccia pore-filling composed of a mixture of detrital and crystal calcite silt, silt-sand sized quartz grains, and insoluble residue material. Crossed polarized light. (E–G) Fissure-filling cements found within breccia-clasts. Some fissures are cemented with ferroan calcite spar (blue) and some with non-ferroan calcite spar (red) indicating different stages of cementation. Fissures cemented with non-ferroan calcite spar are found only within the clasts and are inherited from host rocks as a result of prebrecciation processes. Note that the fissure filled with ferroan calcite spar transects the fissure filled with non-ferroan calcite spar indicating its later origin (E) and that fissures filled with blueish stained calcite spar can cut both the clasts and the matrix (F, G). Micro-breccia material between larger grains is also visible, upper left in (F) and lower part in (G). Micro-breccia material is interpreted as a result of rebrecciation processes related to tectonic and burial stress released during the late diagenetic phase. Pore spaces within the micro-breccia are completely filled with ferroan (blue) detrital calcite silt (lower part in G). Plane-polarized light. Stained with Alizarin red S and K-ferricyanide. (H) Example of breccia pore-geopetal infill where detrital calcite silt occupies the lower part of the pore representing the earlier fill regarding the calcite spar above (central part). Other pores are completely filled with detrital calcite silt (upper left). Blue colour of calcite spar and detrital calcite silt after treatment with Alizarin red S and K-ferricyanide indicating their ferroan nature and late diagenetic, burial origin. Plane-polarized light. Stained with Alizarin red S and K-ferricyanide.

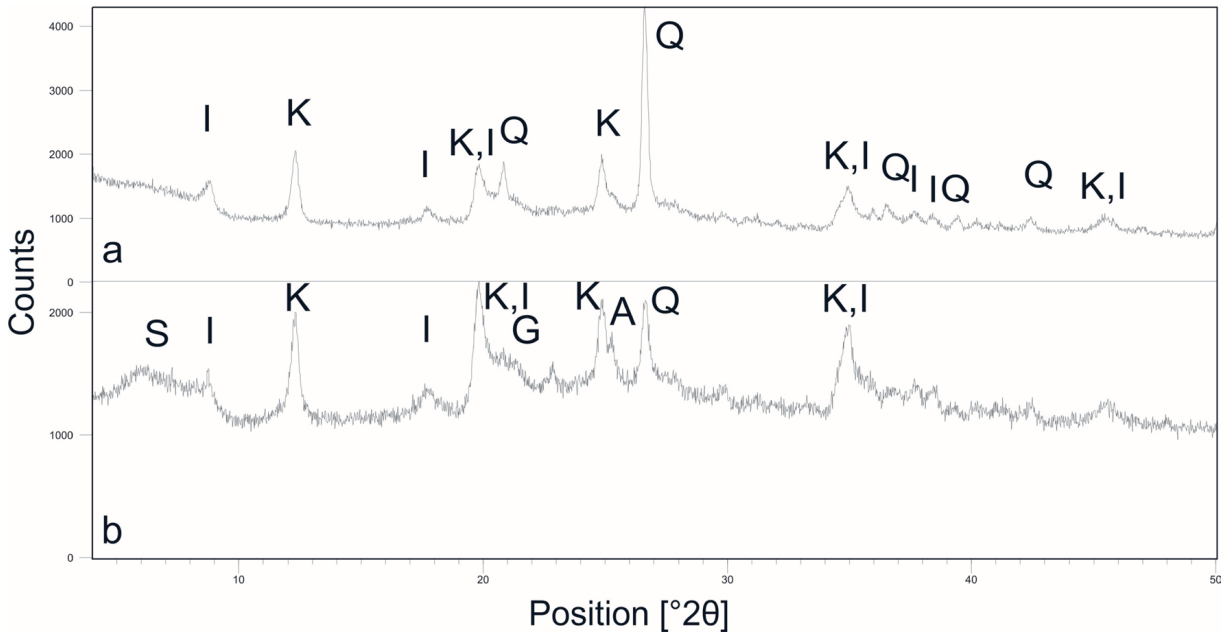

Figure 6. XRD patterns of insoluble reisdues of a breccia clast [a], and whole breccia [b]. A – anatase, G- goethite, I – illite, K – kaolinite, Q – quartz, and S – smectite. Cu Kα radiation.

The intergranular pores and fissures within the breccia are cemented, but in some original pore spaces where spar fill is absent or incomplete the pores are now: a) completely or partially filled with cement crystals or detrital calcite silt (Fig. 5A, B); b) filled with a reddish/yellowish-brown mixture of detrital calcite silt, silt/sand-sized quartz grains, and with a material that is assumed to be insoluble residue (Fig. 5D); or c) filled with reddish/yellowish-brown mixture of fine- to micro-breccia and detrital calcite silt (Figs. 4C, 5F–H). Where calcite cement and detrital silt occur together within a void, the detrital silt either fills the centre, uncemented part of voids (Fig. 5B), representing a later filling episode, or geopetally occupies the lower part of the voids, representing the earlier fill event before the overlying cement precipitated (Fig. 5H). Calcite spar, as well as calcite detrital silt, filling intergranular pores and fissures within the breccias, turns blue after Alizarin red S and potassium ferricyanide treatment indicating the cements are ferroan. These cements are predominantly equant ferroan-calcite spar with drusy fabric characterized by crystal size increasing towards the cavity centre (Fig. 5B). Crystals may reach nearly 1 mm in diameter in the centre of the cavities. Fissures within the breccia with ferroan calcite fill, are located within the clasts, but also extend through the lithified matrix, cutting both the clasts and the matrix (Fig. 5F, G). On the other hand, there are fissures and dissolution-widened cavities that are confined within the clasts that reveal cementation with non-ferroan drusy mosaic calcite spar and detrital calcite-silt fill (Fig. 5C). Geopetally arranged infills of such cavities in different clasts show up orientations that vary indicating some rotation of clasts and therefore the deposition of cavity-infills before brecciation. Also, fissures filled with ferroan calcite spar transect the fissure filled with non-ferroan calcite spar, indicating a later origin for the ferroan calcite fill (Fig. 5E).

Recognition of identical fissures and dissolution-cavities within the host rock characterized by the presence of the non-ferroan calcite spar and/or detrital silt and by the identical infill pattern indicates that the same type of cavities and associated cementation patterns found within clasts were formed in the original host rock, during earlier near-surface diagenesis of host rocks that were later brecciated.

The insoluble residue content of the limestones that host the breccia and of individual clasts that were separated from breccia averages 1%. The insoluble residue content of the breccias as a whole is three times greater. XRPD analyses show that insoluble residues of host rock and separated breccia clasts contain quartz, kaolinite, and illitic material while the dominant mineral phases in the insoluble residues of breccias are quartz, kaolinite, illite, and goethite, with haematite, smectite, and anatase being present in subordinate amounts (Fig. 6). XRPD analysis of the matrix as a whole showed that calcite is the dominant constituent, while quartz, anatase, goethite, and illite are present as minor or trace components. It was very difficult to collect enough pure sample of the matrix to obtain the appropriate amount of insoluble residue for XRPD analysis because of the specific occurrence of the matrix as a thin coating around the grains and its high calcitic composition. Therefore, the composition of the insoluble residue of the matrix was deduced by combining the results of XRPD analyses of the insoluble residue of clasts and breccias and of XRPD analysis of the matrix as a whole. Accordingly, the mineral composition of the insoluble residue of the matrix is quartz, goethite, haematite, smectite, anatase, and illite.

6. DISCUSSION

Many authors have written about the appearance of local and regional palaeokarstic periods and breccias in the AdCP area during the Late Cretaceous and Palaeogene, providing different interpretations as to their origin (e.g. PRTOLJAN & GLOVACKI JERNEJ, 1994; DURN et al., 2003; OTONIČAR, 2007; KORBAR, 2009; VENTURINI & TENTOR, 2010; BRLEK et al., 2013; PEH & KOVAČEVIĆ GALOVIĆ, 2016; OTONIČAR, 2016). However, based on the geological setting and stratigraphic position of the Pag Town breccia body (Figs. 1, 2), its textural and structural characteristics such as chaotic appearance and random fabric, very poorly sorted material, angular fragments, composition reflecting only the host rock lithology, we present two genetic

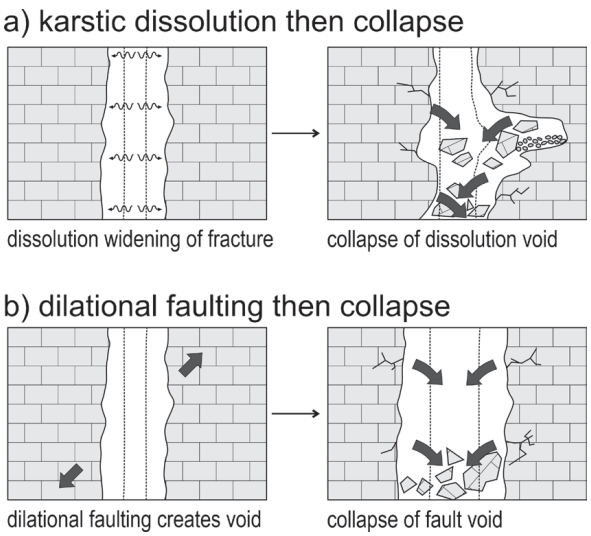

Figure 7. Schematic diagram of the two possible genetic concepts of breccia origin discussed in the paper (modified after WOODCOCK et al., 2014).

scenarios or concepts for the origin of this breccia body (Fig. 7). The first concept involves host rock dissolution resulting in a widened dissolution cavity into which wall and roof rocks progressively collapsed and detrital sediment was imported (Fig. 7a), as described by many authors (e.g. CHOQUETTE & JAMES, 1988; KERANS, 1988, 1993; LOUCKS, 1999; COOPER & KELLER, 2001; LOUCKS, 2007). An alternative scenario involves the origin of the breccia by collapse of voids produced by dilational fault displacement (Fig. 7b), or by a mismatch of fault walls (e.g. WOODCOCK et al., 2006; WOODCOCK et al., 2014). Thus, both concepts assume the gravitational collapse of blocks and slabs into an open void. The size of the original void may be the same as the breccia body, but it is typically smaller since the brecciated zone following collapse usually becomes wider than the original void (LOUCKS, 1999). The question is whether the void originated by karstic dissolution or by extensional/transtensional tectonics. Regardless of which mechanism led to the formation of the breccia body, its characteristics today are mashed, more or less masked, and overprinted by polyphase tectonic and diagenetic alterations.

6.1. Karstic dissolution and collapse scenario

PALMER (1991) used a database of approximately 500 caves to develop statistics on the relative abundance of different modern cave system types. He concluded that approximately 92% of all cave types are products of near-surface karst processes (epigenic cave systems). ESTEBAN (1991) noted that extensive palaeokarst is more commonly associated with composite unconformities than with a single unconformity. Composite unconformities represent long exposure times that may be more than 4 Ma in duration and may coincide with two or more third-order regressive cycles. A new cycle of karst will develop during each cycle of exposure, and each newer karst cycle will overprint the previous cycle. An older system may be abandoned and collapse and then be overprinted by one or more younger systems (LOUCKS, 1999). However, extensive palaeokarsts could also be related to a single unconformity, a good example being the Cretaceous-Palaeogene palaeokarst phase of the AdCP (OTONIČAR, 2007). It is also possible that long-lasting palaeokarsts show less pronounced palaeokarst features than shorter-lasting palaeokarsts (MELIM et al., 2002).

The Upper Cretaceous host rocks in the studied area, as well as in the entire area of the AdCP, were exposed to subaerial, near-surface processes during the Late Cretaceous–Early Eocene regional emersion phase (e.g. JELASKA et al., 1994; ĆOSOVIĆ et

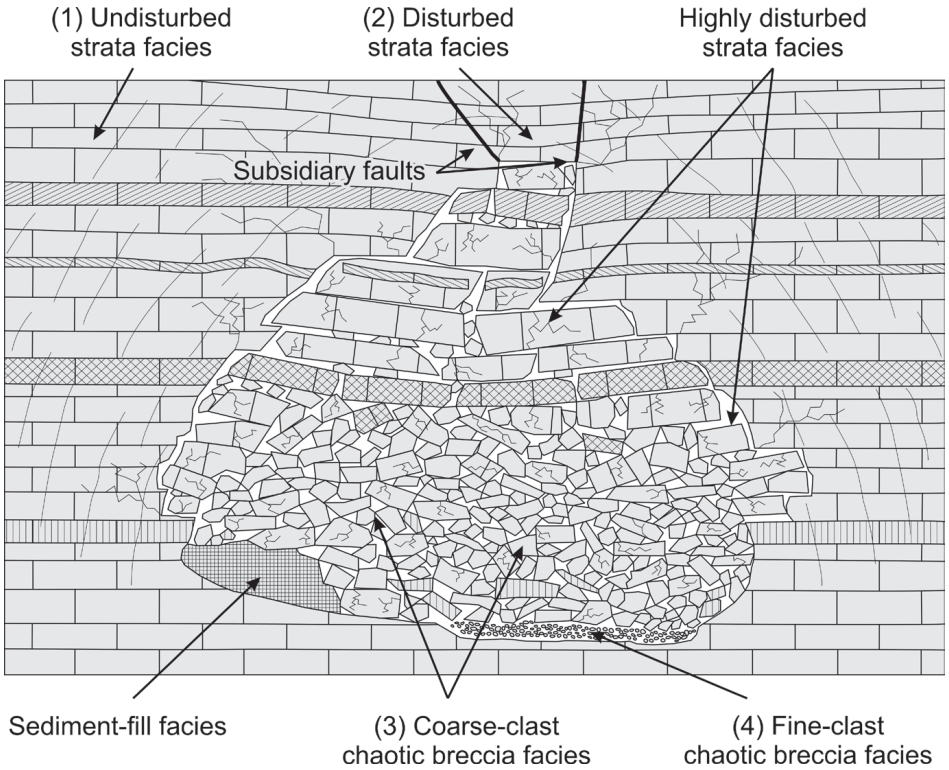

Figure 8. Model showing the final stage of cave collapse during burial with six basic cave facies recognized by rock fabric and structures (modified after LOUCKS & MESCHER, 2001). Numbered facies refer to those found in the study area. Subsidiary faults could be a secondary effect of movement on the main fault or could be attributed to suprastratal deformations that occur as a result of the final collapse during burial.

al., 1994; MATIČEC et al., 1996, CVETKO TEŠOVIĆ et al., 2020). The duration of the emersion phase was different on various parts of the platform, ranging from 0 Ma to 90 Ma (KORBAR, 2009; ŠPANIČEK et al., 2017; OTONIČAR, 2007; PEH & KOVAČEVIĆ GALOVIĆ, 2016), but in the studied area it lasted at least ca. 25Ma (KORBAR, 2009).

In the studied area, the Lower Eocene foraminiferal (alveolinid) limestones were also subjected to a significant local emergence event of indefinite duration (local tectonic uplift?), that is clearly observed within the exposed Lower Eocene shallow-water carbonate sequence. These two emergence occurrences lasted longer than 25 Ma, which corresponds to ESTEBAN's (1991) criterion of long-term exposure of 4 Ma. During each period of such prolonged subaerial exposure, the preburial cave of a near-surface karst environment could enlarge and partly collapse and fill with the debris of the surrounding host rock. The features such as microkarstic voids partially filled with internal sediment (Fig. 5C), dissolution enlargements of tectonically induced fractures, and reddish (haematitic) colouration frequently found within the Upper Cretaceous rocks and within the numerous breccia fragments, are clear indications of the subaerial exposure and dissolution of the Upper Cretaceous host rock. In addition, a very common occurrence of fissures in numerous breccia fragments that are inherited from the host rocks indicates some Late Cretaceous tectonic stresses prior to brecciation processes (Fig. 5E–G). This could lead to easier and more efficient dissolving-fluid activity when significant karstification processes took place and eventually could lead to extensive void formation. Indubitably, all these features visible in numerous breccia fragments indicate that near-surface dissolution processes preceded the brecciation in the study area. This appears to be the case that is common in long-term composite unconformities where there is more than one karst event.

The presence of insoluble residue material incorporated into the breccia matrix, and a mineralogy strongly correlated with the insoluble residues of the host rocks, also suggests that dissolution processes were most likely involved in breccia formation.

LOUCKS & MESCHER (2001) proposed a classification of six common palaeocave facies (Fig. 8). Four of them can be recognized within the studied breccia body so their presence may be evidence of the karstic dissolution and collapse scenario. These are:

(1) Undisturbed strata, which are interpreted as undisturbed host rock (Fig. 4D). In this facies, bedding continuity can be traced even for tens of hundreds of metres.

(2) Disturbed host rock strata around the collapsed passage (Fig. 4E). Here, the bedding continuity is high, but it is weakly folded and offset by small faults. It is commonly overprinted by crackle and mosaic brecciation.

(3) Coarse-clast chaotic breccia is interpreted as collapsed-breccia cavern fill produced by ceiling and wall collapse (Figs. 3A–F, 4B). It is characterized by a mass of very poorly sorted, granule- to boulder-sized chaotic-breccia clasts that can be graded. It is commonly clast supported but can contain matrix material.

(4) Finer-clast stratified chaotic breccia (Fig. 4A) interpreted as hydrodynamically sorted, transported-breccia cavern fill characterized by a mass of clast-supported, moderately sorted granule- to cobble-sized clasts with varying amounts of the matrix. Clasts can be imbricated.

Furthermore, the textural and structural characteristics of the breccia body indicate that the transport distance of the breccia fragments was very short (mosaic breccia with short gravitational displacement with or without rotation of fragments; Fig. 3E) or, in places, there is practically a complete absence of any transport at all (highly fractured crackle breccia; Fig. 3D).

Also, the appearance of breccia intervals displaying the sedimentary structures such as inverse grading, stratification, imbrication, and obstacle marks (Fig. 4A, B, F) indicate void sediment fills deposited by hydrodynamically induced processes such as traction by subterranean streams or mass-flow mechanisms (LOUCKS, 1999). Based on the presence of these features that can only occur in an open space, there had to be a cavern connected to the surface within the Upper Cretaceous carbonate succession.

The presence of sporadic pebble-sized fragments of Lower Eocene foraminiferal (alveolinid) limestone in the central part of the breccia body, a few tens of metres below the Lower Eocene succession, can only be explained by the presence of underground voids/channels. After the lithification of the Lower Eocene limestone, thin vadose karst channels/cracks cut through the underlying layers, large enough only for transport of pebble-sized lithified Lower Eocene limestone clasts into the subsurface void before the final cave roof collapse during burial.

Nevertheless, if we consider a karstic solution and collapse scenario during the long-lasting Late Cretaceous–Early Eocene emersion and subsequent short-lasting Early Eocene emersion, some of its features may be controversial. One of the controversies is reflected in the fact that if such a big underground void existed and extended more than a few tens of metres below the Late Cretaceous/Early Eocene palaeokarstic surface, one would expect at least some cave phenomena visible among the void breccia fragments, i.e., various allogenic and autogenic cave phenomena - speleothems such as flowstones or some bauxite clasts formed on the palaeokarst surface. No such underground or surface palaeokarstic features can be found, neither near the studied breccia body nor within its fragments. But actually, speleothems and bauxite deposits are not commonly expected in caves. Many modern caves today have no or rare speleothems so the lack of speleothems is a poor criterion for interpreting a non-karst origin. LOUCKS (1999) has observed that speleothems could occlude a relatively minor fraction of pore volume in the whole cave system. PALMER (1995) also referred to a similar observation of the lack of speleothems from his studies. FORD & WILLIAMS (1989) noted that some caves are totally devoid of speleothems, whereas in other caves they may be common. Speleothems, therefore, should not be expected as obligatory defining characteristics for all palaeocave systems; however, where they are encountered in the ancient stratigraphic record, they are good indicators of karst processes. With regard to the lack of bauxite fragments, the mineral composition of the surrounding strata should be taken into consideration. Since the host rocks are 99% calcite, their insoluble residues could make little contribution to the formation of bauxite, although conditions for intense leaching were present because of the active vertical drainage through fractured limestones. The aluminosilicate-rich parent material should be present for extensive bauxite formation. In a pure limestone terrain such as this, the aluminosilicate-rich material is present only in a very small amount. Therefore, the accumulation of such material is usually sporadic and localized, so bauxite formation was not expected to occur everywhere on the emergent surfaces.

Furthermore, the fact that the final void collapse in this scenario occurred during burial can also be quite controversial. Usually, cave ceilings become less stable closer to the surface because

a rock-ceiling beam may lose support especially if there are numerous fractures in the ceiling. Such a cantilevered rock beam across a cave ceiling is able to resist gravitational stress in direct proportion to its thickness and inversely proportional to its length (WHITE & WHITE, 1969). That is why there are numerous examples of caves as stable forms deep below the surface, even from the Dinarides. Although palaeocaves are able to resist overburden pressure, they are also affected by tectonic stresses that can trigger cave collapse even in the subsurface burial environment. Movements of the neighbouring main strike-slip fault (Fig, 1B) have the potential to act in the same way.

Emphasized form-fitting fabric, extensive convex-concave and sutured contacts between grains, as well as pressure solution seams, stylolites, and numerous fissures cemented with a ferroan-calcite spar of drusy mosaic fabric, indicate a strong influence of secondary diagenetic processes during burial on producing the final breccia features visible today. Indirectly, this also implies the absence of extensive early near-surface breccia-cementation, as its presence would reduce the impact of later mechanical and chemical compaction.

6.2. Dilational-fault void and collapse scenario

It is very intriguing that a dilational faulting and collapse scenario could also produce the same types of breccia (WOODCOCK et al., 2006; MORT & WOODCOCK, 2008; WOODCOCK & MORT, 2008; WOODCOCK et al., 2014). Several faults are visible in the studied area. One of the faults intersects and displaces the northern, uppermost part of the breccia body and represents a fault with vertical and horizontal displacement (Fig. 1B). Since it intersects the breccia body, it must have been formed after brecciation, so it could not have influenced the formation of the breccia body. Two minor faults striking NE - SW bound the northern margin of the breccia within the Upper Cretaceous strata and another one does not cut the breccia body (Fig. 1B); therefore, these faults cannot be involved in the formation of the breccia either. The main fault, a left-lateral strike-slip fault, separates the Upper Cretaceous and Eocene deposits (Fig. 1B) and is not in contact with the breccia body. It could be assigned to the main Dinaridic thrust-related deformation event where the complex tectonic structure of the whole region was formed that occurred during the Palaeogene (AUBOUIN et al., 1970; CHOROWITZ, 1977; CADET, 1978; PAMIĆ et al., 1998; TARI, 2002; SCHMID et al., 2004). Although this fault may have had the potential for producing brecciation along the fault plane, there is no visible brecciated zone immediately adjacent to the fault line. Fault influence is also questionable because it is not in direct contact with the breccia body. Nonetheless, the proximity of this major strike-slip fault might have affected the surrounding rock. Although this fault is not in direct contact with the breccia body, movements along its main slip surface could affect the neighbouring strata and trigger successive void collapses in both near-surface and subsurface areas. However, in any case, that does not imply the conclusion that this particular fault is responsible for the creation of the void. In addition, minor faults near this main fault could be attributed to subsidiary faults as a secondary effect of the movement on the main fault or be assigned to suprastratal deformations occurring because of final collapse during burial (LOUCKS, 2007) (Fig. 8). As the cavity collapsed during burial, overlying strata could sag or subside over the collapsed area, providing potential for the development of a fracture/fault system that can extend upwards from the collapsed interval. This effect is recorded at horizons more than 800 m above the cavity (LOUCKS, 1999, 2007).

Thus, if we consider such a dilational faulting and collapse scenario during the main Paleogene Dinaridic thrust deformations, a controversy also arises. That is, if the studied breccia body was formed exclusively by the gravitational collapse of a fault-void or by direct fault fragmentation, the geometry of the breccia body should be conformable and parallel with the fault line (COOPER & KELLER, 2001; WOODCOCK et al., 2014). Here, however, there are no visible faults striking parallel to the breccia body. In addition, the absence of some other indicators of collapse into fault-induced voids, such as clasts of crackle and mosaic breccia in the chaotic breccias, representing fragments of faulted wall rock collapsed into the fault void and slickensided clasts from the fault walls (WOODCOCK et al., 2014), further excludes the possibility of such a scenario. Irregular margins and irregular quasi-circular breccia-body geometry, inconsistent with bedding, additionally do not support the scenario of dilational faulting and collapse. In contrast, it is a regular and common feature of dissolution processes to form the voids for subsequent breccia infill (COOPER & KELLER, 2001; WOODCOCK et al., 2014).

7. CONCLUSION

If we consider the pros and cons for the two presented/discussed scenarios, the conclusion arises that the karst dissolution and collapse scenario is the most probable scenario for the Pag Town breccia origin. Except for the fact that dilational-fault void collapse can produce the same type of breccia as karst dissolution void collapse, no other breccia features support the dilational faulting and collapse scenario for the Pag Town breccia origin. Taking into account all of the data presented, the formation of the Pag town breccia can be interpreted as follows. During the emersion phase from the Late Cretaceous to the Early Eocene, the karstification of the exposed Upper Cretaceous host rock occurred, accompanied by intense local fracturing. The fractures allowed easier and more intense penetration of fluids into the host rock, resulting in intense host rock (limestone) dissolution. The resulting and expanding subsurface void in the preburial phase was gradually and partially filled with Upper Cretaceous limestone fragments, both from its ceiling and walls. These rock fragments were even partially transported along the void by mass flow mechanisms and subsurface currents, resulting in clearly visible inverse grading, stratification, imbrication, and obstacle marks. During the Early Eocene, another local emergence of an undetermined duration occurred. At that time, when the cave was only partially filled, only sporadic pebbles of lithified foraminiferal limestone of the Early Eocene age entered the subsurface void through the narrow passages. Thus, in preburial, near-surface conditions during each phase of prolonged subaerial exposure the subsurface void developed and partly collapsed. As burial progressed, the cracked roof of the void eventually collapsed and completely filled the remaining open space (Fig. 8), burial cementation with ferroan calcite spar occurred, mechanical compaction increased, and restructured the breccia fragments and remaining cavities. Continued burial led to further extensive mechanical and chemical compaction resulting in expressive, form-fitting structures, formation of stylolites, and rebrecciation/refragmentation of some clasts leading to the formation of a fine- to microbrecciated matrix. In addition to gravitational stresses caused by the weight of the overlying strata, tectonic stresses induced by the movements of the adjacent main strike-slip fault may have been the trigger for the collapses near the surface and especially in the subsurface.

REFERENCES

AUBOUIN, J., BLANCHET, R., CADET, J.-P., CELET, P., CHARVET, J., CHOROWICZ, J., COUSIN, M. & RAMPNOUX, J.-P. (1970): Essai sur la géologie des Dinarides.– Bull. Soc. Géol. Fr. Sér., 7, 12, 1060–1095. doi: 10.2113/gssgfbull.S7-XII.6.1060

BABIĆ, LJ. & ZUPANIČ, J. (2016): The youngest stage in the evolution of the Dinaric Carbonate Platform: the Upper Nummulitic Limestones in the North Dalmatian foreland, Middle Eocene, Croatia.– Nat. Croat., 25/1, 55–71. doi: 10.20302/NC.2016.25.3

BRINDLEY, G.W. & BROWN, G. (1980): Crystal structures of clay minerals and their X-ray identification.– Min. Soc., London, 495 p. doi: 10.1180/mono-5

BRLEK, M., KORBAR, T., CVETKO TEŠOVIĆ, B., GLUMAC, B. & FUČEK, L. (2013): Stratigraphic framework, discontinuity surfaces, and regional significance of Campanian slope to ramp carbonates from central Dalmatia, Croatia.– Facies, 59, 779–801. doi: 10.1007/s10347-012-0342-0

BROWN, G. (1961): The X-ray identification and crystal structures of clay minerals.– Min. Soc., Clay Minerals Group, London, 544 p.

CADET, J.P. (1978): Essai sur l'évolution alpine d'une paléomarge continentale; les confi ns de la Bosnie-Herzegovine et du Monténegro (Yougoslavie).– Mem. Soc. Geo. F., 133, 1−83.

CHANNELL, J.E.T., D'ARGENIO, B. & HORVÁTH, F. (1979): Adria, the African promontory, in Mesozoic Mediterranean palaeogeography.– Earth-Sci Rev., 15/3, 213−292. doi: 10.1016/0012-8252(79)90083-7

CHOQUETTE, P.W. & JAMES, N.P. (1988): Introduction.– In: JAMES, N.V. & CHOQUETTE, P.W. (eds.): Paleokarst, 1−21, Springer, New York.

CHOROWITZ, J. (1977): Etude geologique des Dinarides le long de la structure transversale Split-Karlovac (Yugoslavie).– Unpubl. Ph. D. thesis, Publ. Soc. Geol. Nord, Villeneuve d Ascq., 11, 1−331.

COOPER, J.D. & KELLER, M. (2001): Paleokarst in the Ordovician of the southern Great Basin, USA: implications for sea-level history.– Sedimentology, 48, 855−873.

CVETKO TEŠOVIĆ, B., MARTINUŠ, M., GOLEC, I. & VLAHOVIĆ, I. (2020): Lithostratigraphy and biostratigraphy of the uppermost Cretaceous to lowermost Palaeogene shallow-marine succession: top of the Adriatic Carbonate Platform at the Likva Cove section (island of Brač, Croatia).– Cretaceous Research, 114, 104507. doi: 10.1016/j.cretres.2020.104507

ĆOSOVIĆ, V., BALONČIĆ, D., KOIĆ, M., MARJANAC, T., MORO, A., GUŠIĆ, I. & JELASKA, V. (1994): Paleontological evidence of Paleogene transgression on Adriatic carbonate platform.– Geol. Mediterr., 21/3–4, 49–53.

DAVIES, W.E. (1949): Features of cave breakdown.– National Speleothem Society Bulletin, 11, 34–35.

DICKSON, J.A.D. (1966): Carbonate identification and genesis as revealed by staining.– J. Sediment. Petrol., 36/2, 491−505.

DROBNE, K., VLAHOVIĆ, I., TRUTIN, M., PAVLOVEC, R., ĆOSOVIĆ, V., BABAC, D., CIMERMAN, F., LUČIĆ, D. & PAVŠIČ, J. (1991): Excursion B – Ravni Kotari, Paleogene.– In: VLAHOVIĆ, I. & VELIĆ, I. (eds): Some Aspects of the Shallow-water Sedimentation on the Adriatic Carbonate Platform (Permian to Eocene), 2nd International Symposium on the Adriatic Carbonate Platform, Excursion Guidebook. Institute of Geology, Zagreb, 53–70.

DURN, G., OTTNER, F., TIŠLJAR, J., MINDSZENTY, A. & BARUDŽIJA, U. (2003): Regional Subaerial Unconformities in Shallow-Marine Carbonate Sequences of Istria: Sedimentology, Mineralogy, Geochemistry and Micromorphology of Associated Bauxites, Palaeosols and Pedo-sedimentary Complexes.– In: VLAHOVIĆ, I. & TIŠLJAR, J. (eds): Field trip guidebook: Evolution of depositional environments from the Palaeozoic to the Quaternary in the Karst Dinarides and the Pannonian Basin, 22nd IAS Meeting of Sedimentology, Institute of Geology, Zagreb, 209–255.

ESTEBAN, M. (1991): Palaeokarst: practical applications.– In: WRIGHT, V.P., ESTEBAN, M. & SMART, P.L. (eds.): Palaeokarst and palaeokarstic reservoirs: University of Reading, Postgraduate Research for Sedimentology, PRIS Contribution No. 152, 89−119.

EVAMY, B.D. (1969): The precipitational environment and correlation of some calcite cements deduced from artificial staining.– J. Sediment. Petrol., 39/2, 787−821.

FERRILL, D.A., WYRICK, D.Y. & SMART, K.J. (2011): Coseismic, dilational-fault and extension-fracture related pit chain formation in Iceland: Analog for pit chains on Mars.– Lithosphere, 3/2, 133–142. doi: 10.1130/L123.1

FORD, D.C. & WILLIAMS, P.W. (1989): Karst geomorphology and hydrology.– Unwin Hyman, London, 601 p. doi: 10.1007/978-94-011-7778-8

GUŠIĆ, I. & JELASKA, V. (1990): Stratigrafija gornjokrednih naslaga otoka Brača u okviru geodinamske evolucije Jadranske karbonatne platforme (Upper Cretaceous stratigraphy of the Island of Brač within the geodynamic evolution of the Adriatic Carbonate Platform).– Opera Acad. sci. art. Slav. merid. Zagreb, 69, 160 p.

GUŠIĆ, I. & JELASKA, V. (1993): Upper Cenomanian-Lower Turonian sea-level rise and its consequences on the Adriatic-Dinaric carbonate platform.– Geol. Rundsch., 82/4, 676−686. HIGGINS, M. W. (1971): Cataclastic rocks.– Prof. Pap. U.S. Geol. Surv., 687, 97p.

JELASKA, V., GUŠIĆ, I., JURKOVŠEK, B., OGORELEC, B., ĆOSOVIĆ, V., ŠRIBAR, L. & TOMAN, M. (1994): The Upper Cretaceous geodynamic evolution of the Adriatic–Dinaric carbonate platform(s).– Geol. Mediterr., 21/3–4, 89–91. doi: 10.3406/geolm.1994.1534

JELASKA, V. (2003): Carbonate Platforms of the External Dinarides.– In: VLAHOVIĆ, I. & , J. (eds.): Evolution of depositional environments from the Palaeozoic tothe Quaternary in the Karst Dinarides and the Panonian Basin. 22nd IAS Meeting of Sedimentology. Field Trip Guidebook, 67−71 p.

JENKYNS, H.C. (1991): Impact of Cretaceous sea level rise and anoxic events in the Mesozoic carbonate platform of Yugoslavia.– Am. Assoc. Pet. Geol. B., 75, 1007−1017.

KAUFMAN, G. & BRAUN, J. (2000): Karst aquifer evolution in fractured, porous rocks.– Water resources research, 36/6, 1381–1391. doi: 10.1029/1999WR900356

KERANS, C. (1988): Karst-controlled reservoir heterogeneity in Ellenberger Group carbonates of west Texas.– Am. Assoc. Petr. Geol. B., 72, 1160−1183.

KERANS, C. (1993): Description and interpretation of karst-related breccia fabrics, Ellenburger Group, west Texas.– In: WILSON, J.L. & YUREWICZ, D.A. (eds.): Paleokarst Related Hydrocarbon Reservoirs, 18, SEPM Core Workshop, 181−200.

KORBAR, T. (2009): Orogenic evolution of the External Dinarides in the Adriatic region: a model constrained by tectonostratigraphy of Upper Cretaceous to Paleogene carbonates.– Earth-Sci. Rev., 96, 296−312. doi: 10.1016/j.earscirev.2009.07.004

KOŠIR, A. (1997): Eocene platform-to-basin depositional sequence, southwestern Slovenia.– Gaea Heidelbergiensis, 3, 205 p.

LAZNICKA, P. (1988): Breccias and coarse fragmentites: Petrology, environments, associations, ores.– Developments in Economic Geology, 25, 351 p.

LOUCKS, R.G. (1999): Paleocave carbonate reservoirs: origins, burial-depth modifications, spatial complexity, and reservoir implications.– Am. Assoc. Petr. Geol. B., 83, 1795−1834.

LOUCKS, R.G. (2007): A Review of Coalesced, Collapsed-Paleocave Systems and Associated Suprastratal Deformation.– Acta Carsologica, 36/1, 121–132. doi: 10.3986/ac.v36i1.214

LOUCKS, R.G. & HANDFORD, R.H. (1992): Origin and recognition of fractures, breccias, and sediment fills in paleocave-reservoir networks.– In: CANDELARIA, M.P. & REED, C.L. (eds.): Paleokarst, karst related diagenesis and reservoir development: examples from Ordovician-Devonian age strata of West Texas and the Mid-Continent: Permian Basin Section, SEPM Publication, 92–33, 31−44.

LOUCKS, R.G. & MESCHER, P. (2001): Paleocave facies classification and associated pore types.- Am. Assoc. Petr. Geol., Southwest Section, Annual Meeting, Dallas, Texas, CD-ROM, 18.

MAJCEN, Ž., KOROLIJA, B., SOKAČ, B. & NIKLER, L. (1970): Osnovna geološka karta SFRJ 1:100000, list Zadar L 33–139 [*Basic Geological Map of SFRY 1:10000, Zadar sheet* – in Croatian].– Inst. geol. istraživanja, Zagreb, Savezni geološki zavod, Beograd.

MAMUŽIĆ, P., SOKAČ, B. & VELIĆ, I. (1970): Osnovna geološka karta SFRJ 1:100000, list Silba L 33–126 [*Basic Geological Map of SFRY 1:100000, Silba sheet* – in Croatian].– Inst. geol. istraživanja, Zagreb, Savezni geološki zavod, Beograd.

MARJANAC, T. & ĆOSOVIĆ, V. (2000): Tertiary Depositional History of Eastern Adriatic Realm.– Vijesti Hrvatskoga geološkog drustva, 37, 93–103.

MATIČEC, D., VLAHOVIĆ, I., VELIĆ, I. & TIŠLJAR, J. (1996): Eocene limestones overlying Lower Cretaceous deposits of western Istria (Croatia): did some parts of present Istria form land during the Cretaceous?– Geol. Croat., 49/1, 117–127.

MELIM, L.A., WESTPHAL, H., SWART, P.K., EBERLI, G. & MUNNECKE, A. (2002): Questioning carbonate diagenetic paradigms: evidence from the Neogene of the Bahamas.– Mar. Geol., 185, 27–53. doi: 10.1016/S0025-3227(01)00289-4

MOORE, D.M. & REYNOLDS, R.C. (1997): X-Ray Diffraction and the Identification and Analysis of Clay Minerals.– Oxford University Press, Oxford, 378 p.

MORT, K. & WOODCOCK, N.H. (2008): Quantifying fault breccia geometry: Dent Fault, NW England.– J. Struct. Geol. 30, 701–709. doi: 10.1016/j.jsg.2008.02.005

OTONIČAR, B. (2007): Upper Cretaceous to Paleogene Forbulge Unconformity Associated with Foreland Basin Evolution (Kras, Matarsko Podolje and Istria; SW Slovenia and NW Croatia).– Acta Carsologica, 36/1, 101–120. doi: 10.3986/ac.v36i1.213

OTONIČAR, B. (2016): Stratigraphy and evolution of the forebulge related paleokarst – introduction to excursions A and C.– In: OTONIČAR, B. & GOSTINČAR, P. (eds.): Paleokarst: abstracts & guide book, 24th International Karstological School Classical Karst, Postojna, 42–50.

PALMER, A.N. (1991): The origin and morphology of limestone caves.– Geol. Soc. Am. Bull., 103, 1−21. doi: 10.1130/0016-7606(1991)103%3C0001:OAMOLC%3E2.3.CO;2

PALMER, A.N. (1995): Geochemical models for the origin of macroscopic solution porosity in carbonate rocks.– In: BUDD, D.A., SALLER, A.H. & HARRIS, P.M. (eds.): Unconformities and porosity in carbonate strata: AAPG Memoir, 63, 77–102.

PAMIĆ, J., GUŠIĆ, I. & JELASKA, V. (1998): Geodynamic evolution of the Central Dinarides.– Tectonophysics, 297, 251–268. doi: 10.1016/S0040-1951(98)00171-1

PANALYTICAL (2004): X'Pert HighScore Plus, Version 2.1, Almelo.

PEH, Z. & KOVAČEVIĆ GALOVIĆ, E. (2016): Geochemistry of Lower Palaeogene bauxites – a unique signature for the tectonostratigraphic evolution of part of the Croatian Karst.– Geol. Croat., 69/2, 269–279. doi: 10.4154/gc.2016.24

PRTOLJAN, B. & GLOVACKI JERNEJ, Ž. (1994): On the orgin of the Oklad Breccia on the Island of Brač (Southern Croatia).– Geol. Croat., 47/1, 67–72.

RAMOVŠ, A., HINTERLECHNER-RAVNIK, A., KALENIĆ, M., KARAMATA, S., KOCHANSKY-DEVIDÉ, V., KRSTIĆ, B., KULENOVIĆ, E., MIRKOVIĆ, M., PETKOVSKY, P., SREMAC, J. & TEMKOVA, V. (1990): Stratigraphic Correlation Forms of the Yugoslav Paleozoic.– Rend. Soc. Geol. It., 12, 359−383.

SCHMID, S.M., FÜGENSCHUH, B., KISSLING, E. & SCHUSTER, R. (2004): Tectonic map and overall architecture of the Alpine orogen.– Eclogae Geol. Helv., 97, 93–117. doi: 10.1007/s00015-004-1113-x

SCHMID, S.M., BERNOULLI, D., FÜGENSCHUH, B., MATENCO, L., SCHEFER, S., SCHUSTER, R., TISCHLER, M. & USTASZEWSKI, K. (2008): The Alpine-Carpathian-Dinaridic orogenic system: correlation and evolution of tectonic units.– Swiss J. Geosci., 101, 139–183. doi: 10.1007/s00015-008-1247-3

SCHOLZ, C.H. (1990): The mechanics of earthquakes and faulting.– Cambridge University Press, 442 p.

SOKAČ, B., NIKLER, L., VELIĆ, I. & MAMUŽIĆ, P. (1974): Osnovna geološka karta SFRJ 1:100000, list Gospić L 33–127 [*Basic Geological Map of SFRY 1:100000, Gospić sheet* – in Croatian].– Inst. geol. istraživanja, Zagreb, Savezni geološki zavod, Beograd.

SPRY, A. (1969): Metamorphic Textures.– Pergamon Press, London, 1−350.

SREMAC, J. (2005): Equatorial Shelf of the Palaeozoic Supercontinent – Cradle of the Adriatic Carbonate Platform.– Geol. Croat., 58/1, 1−19. doi: 10.4154/GC.2005.01

ŠPANIČEK, J., ĆOSOVIĆ, V., MRINJEK, E. & VLAHOVIĆ, I. (2017): Early Eocene evolution of carbonate depositional environments recorded in the Čikola Canyon (North Dalmatian Foreland Basin, Croatia).– Geol. Croat., 70/1, 11–25. doi: 10.4154/gc.2017.05

TARI, V. (2002): Evolution of the northern and western Dinarides: A tectonostratigraphic approach.– European Geosciences Union Stephan Mueller Special Publication Series, 1, 223–236. doi: 10.5194/smsps-1-223-2002

TIŠLJAR, J., VLAHOVIĆ, I., VELIĆ, I. & SOKAČ, B. (2002): Carbonate Platform Megafacies of the Jurassic and Cretaceous Deposits of the Karst Dinarides.– Geol. Croat., 55/2, 139–170. doi: 10.4154/GC.2002.14

VELIĆ, I., VLAHOVIĆ, I. & MATIČEC, D. (2002): Depositional sequences and palaeogeography of the Adriatic carbonate platform.– Mem. Soc. Geol. It., 57, 141−151.

VENTURINI, S. & TENTOR, M. (2010): La breccias di Slivia: una testimonianza di eventi paleotettonici Campiano–Maastrichtiano nel Carso Triestino.– Natura Nascosta, 41, 1–15.

VLAHOVIĆ I., TIŠLJAR, J., VELIĆ, I. & MATIČEC, D. (2005): Evolution of the Adriatic carbonate platform; paleogeography, main events and depositional dynamics.– Palaeogeogr. Palaeoclim. Palaeoec., 220, 333–360.

WALKER, R.J., HOLDSWORTH, R.E., IMBER, J. & ELLIS, D. (2011): The development of cavities and clastic infills along fault-related fractures in Tertiary basalts on the NE Atlantic margin.– J. Struct. Geol., 33/2, 92−106. doi: 10.1016/j.jsg.2010.12.001

WHITE, E.L. & WHITE, W.B. (1969): Processes of cavern breakdown.– National Speleothem Society Bulletin, 31, 83–96.

WOODCOCK, N.H. & MORT, K. (2008): Classification of fault breccias and related fault rocks.– Geol. Mag., 145, 435−440. doi: 10.1017/S0016756808004883

WOODCOCK, N.H., OMMA, J.E. & DICKSON, J.A.D. (2006): Chaotic breccia along the Dent Fault, NW England: implosion or collapse of a fault void?– J. Geol. Soc. Lond., 163, 431−446. doi: 10.1144/0016-764905-067

WOODCOCK, N.H., MILLER A.V.M. & WOODHOUSE C.D. (2014): Chaotic breccia zones on the Pembroke Peninsula, south Wales: Evidence for collapse into voids along dilational faults.– J. Struct. Geol., 69, 91−107. doi: 10.1016/j.jsg.2014.09.019